Raman microspectroscopic approach to the study of human granulocytes

G. J. Puppels, H. S. P. Garritsen, G. M. J. Segers-Nolten, F. F. M. de Mul, and J. Greve
Biophysical Technology Group, Faculty of Applied Physics, University of Twente, 7500 AE Enschede, the Netherlands

ABSTRACT A sensitive confocal Raman microspectrometer was employed to record spectra of nuclei and cytoplasmic regions of single living human granulocytes. Conditions were used that ensured cell viability and reproducibility of the spectra.

Identical spectra were obtained from the nuclei of neutrophilic, eosinophilic, and basophilic granulocytes, which yield information about DNA and protein secondary structure and DNA-protein ratio. The cytoplasmic Raman spectra of the three cell types are very different. This was found to be mainly due to the abundant presence of peroxidases in the cytoplasmic granules of neutrophilic granulocytes (myeloperoxidase) and eosinophilic granulocytes (eosinophil peroxidase). Strong signal contributions of the active site heme group(s) of these enzymes were found.

This paper illustrates the potentials and limitations for Raman spectroscopic analysis of cellular constituents and processes.

INTRODUCTION

Raman spectroscopy (RS) has proven to be a powerful method for the characterization of biological molecules (see references 1–3 for reviews). The spectra, which are of a vibrational nature, convey information about the structure and chemical (micro)environment of the molecules and molecular subgroups that are present in a sample. The main disadvantage of RS is the inherently low intensity of the signal obtained. In situ studies of biological molecules at a single cell level have therefore been limited to the case of the highly condensed DNA in salmon sperm cells (4) and to molecules that can be resonantly excited (5–7). The novel sensitive confocal Raman microspectrometer (CRM) developed in our laboratory greatly extends the applicability of RS in this respect. It enables the investigation of single cells and chromosomes with a spatial resolution of $0.45 \times 0.45 \times 1.3\ \mu m^3$ (8, 9).

There are some noticeable differences between working with living cells and working with model systems concerning the way experiments can be carried out and the interpretation of the results. First of all cell viability is a matter of concern which poses limitations on the laser light intensity, the laser wavelength, and the measurement times that can be employed (62). In line with this the choices of these parameters must be such that reproducible spectra can be obtained. In experiments with isolated compounds, potential photochemical, or photothermal effects can often be precluded by employing a flow system instead of a static sample container. Apart from these experimental factors the intrinsic reproducibility of cell spectra will be lower than of isolated compounds because of the simple fact that molecules are not homogeneously distributed throughout the cell. Furthermore the molecular composition of cells or subcellular structures is not precisely known, unlike that of isolated compounds or model systems. The first step in the interpretation of cell spectra is therefore to identify the molecules contributing Raman signal. After that comparisons can be made with spectra of isolated compounds or model systems to learn more about the molecules in their natural environment.

The CRM is presently being used for a RS characterization of white blood cells, as a prelude to studies concerning their functioning in the human immune system. This paper describes a Raman microspectroscopic investigation of human neutrophilic, eosinophilic, and basophilic granulocytes and was carried out along the lines described above. These cells, especially eosinophilic and neutrophilic granulocytes, are from a practical viewpoint very suitable for a compositional and conformational study of chromatin in situ. The position of the nucleus (in the unstained cells) can in general easily be determined because of the dense granulation of the cytoplasm (see, e.g., reference 10). It was furthermore of importance in view of our long term goals to learn whether some of the cytoplasmic compounds of the granulocytes, known to play key roles in defense mechanisms could be traced by means of RS.

Neutrophilic granulocytes are very motile cells that respond to chemotactic stimuli. Their main functions

Address correspondence to Dr. G. J. Puppels, Biophysical Technology Group, Faculty of Applied Physics, University of Twente, P.O. Box 217, 7500 AE Enschede, the Netherlands.

0006-3495/91/11/1046/11 $2.00

are phagocytosis, killing, and digestion of bacteria and other micro organisms. Mature neutrophils have a segmented nucleus. They possess 50–200 cytoplasmic granules of ~0.2 μm in diameter (11) which contain a wide variety of oxidative metabolites and digestive enzymes. Two types of granules are distinguished; azurophilic (or primary) and specific (or secondary) granules. A prominent enzyme of the azurophilic granules is myeloperoxidase (MPO), a heme protein (14). MPO has been reported to make up 5% of a neutrophilic granulocyte's dry weight (12). It catalyzes the oxidation of halide ions to hypohalite, which is cytotoxic to bacteria (13). After phagocytosis these granules fuse with the phagosome upon which degradation of the ingested object commences. Mature neutrophilic granulocytes are deficient in protein synthesis as is evident from the fact that they possess only a few ribosomes and a small endoplasmatic reticulum (14).

Eosinophilic granulocytes are cytotoxic to parasites and play a negative modulatory role in immuno inflammation. Their exact function is not yet understood (13, 15). The nucleus of an eosinophilic granulocyte usually consists of two rounded segments. In the cytoplasm approximately 200 granules are found, with an average diameter of 0.9–1.3 μm (14). These granules contain a crystalloid core, consisting of a single protein, called the Major Basic Protein. The core is surrounded by a less electron-dense granule matrix, in which high concentrations of eosinophil peroxidase (EPO) are found. EPO, like MPO, is a heme protein (15, 16).

Basophilic granulocytes possess granules up to 1.2 μm in diameter (17) which contain large amounts of heparin and histamine (14). Basophilic granulocytes play an important role in hypersensitivity responses (18).

MATERIALS AND METHODS

Sample preparations

Peripheral blood of healthy individuals was obtained by venipuncture. Neutrophilic and eosinophilic granulocytes were isolated as a mixed cell fraction by means of a density gradient method (19).

Basophilic granulocytes were isolated (from the total white blood cell fraction) by means of fluorescence activated cell sorting, after labeling with a human IgE antiserum conjugated to fluorescein (20, 21) (Kent Laboratories Inc., Redmont, WA). The 488 nm line of an Argon-ion-laser was used for fluorescence excitation. 80% pure basophilic granulocyte samples were obtained in this way. During labeling, sorting, further preparation, and RS measurements, the cells were kept at a temperature ≤4°C. The sheet fluid of the flow sorter was also cooled to 4°C. As evidenced by cytospin preparations stained with Wright's stain (22) no degranulation occurred under these conditions. After isolation a drop of cell suspension (neutrophilic granulocytes and eosinophilic granulocytes or basophilic granulocytes) was placed on a poly-*L*-lysine (P-6516; Sigma Chemical Co., St. Louis, MO) coated fused silica substrate, and left to stand for 10 min in a 100% humid environment at room temperature (neutrophilic granulocyte and eosinophilic granulocyte) or at 4°C (basophilic granulocyte). This allowed the cells to attach to the surface of the substrate, which was then placed in a petri dish filled with Hank's Buffered Salt Solution (prepared according to Gibco HBSS nr. 041-04025, phenol-red omitted; Gibco BRL Life Technologies, Brezda, The Netherlands). Raman spectra were measured of the cells on the substrate in the petri dish (to which HBSS-ice cubes were added in the case of basophilic granulocytes). Measurements were carried out within a period of 1–2 h after cell attachment.

Cells of the mixed neutrophilic and eosinophilic granulocyte sample were identified with the CRM in normal light microscopic mode. Eosinophilic granulocytes were distinguished from neutrophilic granulocytes on the basis of their coarser granulation and more prominent nucleus. The classification of the unstained cells was checked and confirmed by staining the cells with Wright's stain, after the RS measurements, and relocalizing them on the substrate.

The 20% impurity in the flow sorted basophilic granulocyte samples consisted of cells belonging to all other white blood cell fractions (i.e., lymphocytes, monocytes, neutrophilic, and eosinophilic granulocytes). Therefore after Raman measurements the cells of these samples were stained and identified as in the case of neutrophilic and eosinophilic granulocytes, to avoid confusion of basophilic granulocyte spectra with spectra of other cells.

A sample of native (oxidized) MPO of 230 μM l^{-1}, isolated from human neutrophilic granulocytes, was a gift of Dr. R. Wever of the University of Amsterdam. It was prepared according to the method described in reference 61. A value of 0.67 was measured for the absorbance ratio A_{428}/A_{280}.

Calf Thymus (CT) DNA (type I, D-1501; Sigma Chemical Co.) was used without further purification and was dissolved in Phosphate Buffered Saline at a concentration of 18 mg/ml (±5%). The concentration was determined by measuring the extinction at 260 nm, using an extinction value of 20 $(mg/ml)^{-1} \cdot cm^{-1}$ (59).

A concentrated CT-Histone II-AS (H-7755, lyophilized; Sigma Chemical Co.) solution in PBS was prepared. The final concentration of dissolved protein was 47 mg/ml (±4%), as determined by the Lowry-Method (25). Solutions of human albumine (A-8763; Sigma Chemical Co.) and of bovine albumine (A-7906; Sigma Chemical Co.) were prepared at concentrations of 80 mg/ml (±4%) and 205 mg/ml (±4%), respectively.

Raman and absorption spectroscopy

All Raman spectroscopic measurements were carried out with the confocal Raman microspectrometer (CRM), described in detail in reference 9. A high numerical aperture microscope objective (63× Zeiss Plan Neofluar water immersion, NA 1.2; Zeiss Nederland B.V., Weesp, The Netherlands) was used for focusing of the laser light in the cells and for collection of the scattered light. The spatial resolution of the CRM is 0.45 · 0.45 · 1.3 μm^3 (1.3 μm along optical axis) (9). Laser light of 660 nm from a Spectra-Physics Analytical (San Jose, CA) 375 B DCM-operated dye laser, was used for excitation. At this wavelength no sample degradation was found to occur in lymphocytes and chromosomes (62). A Wright Instruments Ltd. liquid nitrogen cooled CCD-camera was used for signal detection. Positioning of the cells in the laser focus occurred with the CRM in normal light microscopic mode, using the in-base illumination system of the microscope frame (Nikon Optiphot; Nippon Kogaku K.K., Tokyo).

Raman spectra of MPO were also measured with the CRM with the sample in a circulating flow system. It was pumped at a velocity of ~1 cm/s through a square capillary glass tube with an inner diameter of 500 μm and walls of 100 μm. A 63× Zeiss Plan Neofluar water immersion microscope objective with cover glass correction was used to focus the laser light in the tube and to collect the scattered light.

RS measurements of the DNA and protein solutions were carried out with the samples held in a small plastic container covered by a microscope cover glass. The same objective as used for the MPO measurements was employed. A Raman spectrum of stock solution of the fluorescein-conjugated human IgE antiserum was recorded with the sample in a capillary tube as used for the MPO sample using the same microscope objective.

For all spectra shown, water signal contributions have been subtracted. Wave number calibrations were made on the basis of an indene spectrum recorded at the same setting of the spectrometer as used in the cell measurements. Positions of well-resolved bands are accurate within ± 2 cm^{-1}. The spectra were corrected for the wavenumber-dependent signal detection efficiency of the set up and for pixel-to-pixel variations in detector sensitivity (9).

Absorption spectra were recorded on a Beckmann DU-8 spectrophotometer.

Cell viability

The acridine orange-ethidium bromide method (24) was used to test cell viability, after the measurements.

Determination of DNA-protein ratio

The nuclear Raman spectra that were obtained, contained no discernable signal contributions from other compounds than DNA and protein (see Results). For a determination of the DNA-protein ratio of the chromatin in the granulocyte nuclei we have used the intensities of the 1,094 cm^{-1} B-DNA backbone line and the 1,449 cm^{-1} protein line as internal markers of DNA and protein concentrations, respectively. The intensity of 1,094 cm^{-1} DNA line is virtually insensitive to DNA-protein interactions in nucleosomes and chromatin (26–28) and in DNA-polylysine and DNA-polyarginine complexes (29, 30). The intensity of 1,449 cm^{-1} protein line is insensitive to protein secondary structure and depends only on the number of protein CH_2 and CH_3 groups (2, 40). Assuming that both lines are invariant to intracellular factors (pH, ionic composition) that cannot be controlled in these experiments, the use of these lines as concentration markers seems reasonable. For calibration of these marker lines spectra were measured of a CT-DNA solution (in PBS) and a CT-histone II-AS solution (PBS) of known concentrations (wt/vol). These calibration spectra were subtracted from the granulocyte nucleus spectrum of Fig. 1, scaling in such a way that in the resulting difference spectrum no intensity was found in the 1,094 and 1,449 cm^{-1} lines. The nuclear DNA-protein ratio (wt/wt) was then calculated from the scaling factors applied to the calibration spectra. The estimation of the error in the DNA-protein ratio thus determined was based on the error in the measured concentration of the calibration samples (DNA and protein) and on the uncertainty in the determination of the scaling factors (±5%). The use of human albumine or bovine albumine solutions for protein concentration calibration yielded only slightly different results for the nuclear DNA-protein ratio (in the order of 5%), well within the experimental margin of error.

RESULTS

Raman spectra were obtained from nuclei and cytoplasmic regions of intact human neutrophilic, eosinophilic, and basophilic granulocytes. The fact that the basophilic granulocytes were fluorescently labeled did not interfere with the recording of Raman spectra, because the fluorescein molecules were not excited by the 660 nm laser light (see also Fig. 6).

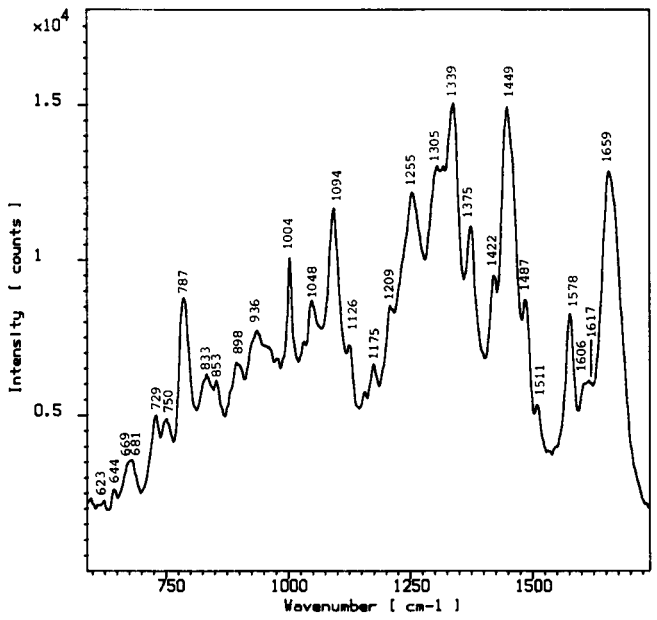

FIGURE 1 Raman spectrum of the nucleus of intact neutrophilic granulocytes. Spectrum averaged over; measurements on different cells. Laser power: 6 mW (660 nm); measuring time: 150 s per measurement.

Fig. 1 shows a neutrophilic granulocyte nuclear spectrum, Figs. 3, 5, and 6 show cytoplasmic spectra. Significance and validity of any (quantitative) interpretation of these spectra depend of course on the reproducibility of the results, both with respect to cell-to-cell and intracellular variations as with respect to possible laser irradiation induced effects. These matters will therefore be discussed first.

Cell viability

It was already shown that lymphocytes survive a 300-s 660-nm laser irradiation at powers up to 20 mW using the same optical configuration as used here (62). In the present investigation a laser power of only 6 mW and measuring times of 30–150 s were used. Viability tests performed on irradiated and unirradiated (control) cells showed no increase in the number of dead cells as a result of the laser irradiation.

Cell viability was typically ~90%, 2 h after attaching the cells to the substrate. The Raman spectra presented here therefore provide information about molecular composition and conformation in living cells.

Reproducibility of spectra

Nuclear region

Spectra obtained from the nuclei of different neutrophilic (neutrophilic granulocyte) and eosinophilic granulocytes (eosinophilic granulocyte) were very reproducible. Fig. 1 shows a neutrophilic granulocyte nuclear spectrum. Slight differences (±10%) in the intensity ratio I_{1094}:I_{1450} (representative of DNA-protein ratio see below) were found. Only the unassigned band at 1,048 cm^{-1} showed a wide variation in intensity, being completely absent occasionally. All nuclear measurements were recorded with 150 s measuring time. Repeated measurements in the same nucleus did not show any changes that would point to the sample integrity being affected by the laser light. Nevertheless the measuring time was limited to 150 s because the cells, even though attached to the poly-L-lysine coated substrates, were able to change in shape (especially neutrophilic granulocytes). Longer measuring times therefore often resulted in spectra containing signal contributions of the cytoplasm too.

Microscope images can be misleading when trying to determine the location of the nucleus in unstained cells. The nuclear and cytoplasmic spectra of neutrophilic granulocytes and basophilic granulocytes both contain a number of strong lines (DNA signal contributions in the nucleus and peroxidase signal contribution in the cytoplasm) specific for those regions of the cells. This provided an intrinsic check for the region inside a cell from where the spectrum was obtained. This was not so clear for measurements on basophilic granulocytes. However, when focusing in the suspected nuclear region, in most cases spectra identical to the nuclear spectra of neutrophilic granulocytes and basophilic granulocytes were obtained. These have therefore been interpreted as basophilic granulocyte nuclear spectra.

Cytoplasmic region

Peroxidase lines in the neutrophilic and eosinophilic granulocyte cytoplasmic spectra were found to slowly decrease in intensity when consecutive recordings were made at the same position in a cell. This is most likely due to photochemical processes (63, 64) caused by the absorption of laser light (see Fig. 4). Using a measuring time of 30 s and a laser power of 6 mW no or only very little changes were observed between the first two spectra recorded at the same position. The measuring time for the neutrophilic and eosinophilic granulocyte cytoplasmic spectra shown in this work was therefore limited to 30 s. The spectra thus obtained were very reproducible. No qualitative differences were observed between spectra obtained from different cells or different cytoplasmic regions within a cell. In eosinophilic granulocyte spectra large variations in the absolute intensity of the Raman lines were found. These are most likely due to variations in the number of granules present in the cytoplasmic regions where spectra were recorded. In unstained eosinophilic granulocytes the granules can be visualized very well. In occasionally seen small cytoplasmic regions lacking granules or containing only a few granules, spectra could be obtained with (almost) no signal contributions of EPO (see Fig. 5).

In basophilic granulocytes no influence of prolonged laser irradiation was observed.

Raman line assignments and interpretation

Spectra obtained from the nucleus and cytoplasmic region of the cells will be discussed separately.

Nuclear spectra. Fig. 1 shows a neutrophilic granulocyte nuclear spectrum averaged over five measurements. As mentioned above only small variations in line intensities were found in separate measurements. Neutrophilic, eosinophilic, and basophilic granulocyte nuclear spectra were found to be indistinguishable. The origin of the 1,048 cm^{-1} line is not clear at this moment (see below). All other lines in the nuclear spectra could be assigned to DNA and protein vibrations (Table 1). Possible RNA (31) and lipid (32, 56, 57) signal contributions are not discernable. The assignments were based on reported RS studies of DNA, nucleosomes, and chromatin (26–28, 33, and references therein).Upon comparison with the spectra in these studies, it appears that in the nuclear spectrum the line-intensity of many DNA-base vibrations relative to the line-intensity of the backbone phosphate vibration at 1,094 cm^{-1} is significantly lower. This is accounted for by the fact that in this work a laser excitation wavelength of 660 nm was used while in the work referred to 514.5 nm laser light was used. In reference 34 it was shown that the relative intensity of base vibrations depends on laser excitation wavelength. This phenomenon was ascribed to preresonance effects. The low intensities of the base-vibration lines, among which the 1,487 cm^{-1} line of guanine, are therefore not the result of DNA-protein interactions (35) in the nucleus. We have so far been unable to assign the 1,048 cm^{-1} line. It is not present in the cytoplasmic spectra. It is also absent from spectra of DNA, nucleosomes, chromatin, metaphase chromosomes, and polytene chromosomes (8, 26–28, 33, 36, 37). This line showed the largest relative variation in intensity of all nuclear Raman lines (occasionally being absent altogether) which may indicate that it does not originate

TABLE 1 **Raman line assignments granulocyte nuclei**

Line position		Assignments (26–28, 33, 60)	
cm^{-1}			
623		phe	
644		tyr	
669		T, G	
681		G ring-breathing	
729		A ring-breathing	
750		T ring-breathing	
783	−787	C ring-breathing, T	
792		DNA:BK:O-P-O symm. str.	
833		DNA:RP, tyr	
853		tyr	p:C-C skeletal modes
898		DNA:BK	
936		p:α-helix	
1004		phe	
1032		phe	
1048		unassigned	
1056		DNA:CO str.	
1094		DNA:BK:O-P-O^- symm. str.	p:C-N str.
1126			
1145		DNA:RP	
1175		tyr, phe	
1209		phe, tyr	
1215		T, C	
1232		C	p:Amide III
1240		T	
1255		A	
1305		A	p:CH def.
1339		A	
1375		T, A, G	
1400		CO_2^-	
1422		A, G	
1449		p:CH-defs.	
1487		G, A	
1511		A	
1578		G, A	
1606		phe, tyr	
1617		tyr, phe	p:Amide I
1659			
1670		T (C = 0)	

Abbreviations: phe, tyr: phenylalanine, tyrosine; p: protein; A, T, G, C: adenine, thymine, guanine, cytosine; sym., asym., str., def.: symmetric, asymmetric, stretching, deformation; BK: backbone.

from a compound or complex evenly distributed throughout the nucleus. A weak line at 1,048 cm^{-1} can be observed in spectra of ribosomal RNA isolated from rat liver (36). As noted before, however, the nuclear spectrum contains no evidence for the presence of RNA.

DNA secondary structure

A number of marker lines has been established for the determination of DNA secondary structure from Raman spectra (33, 37, 38). They show that the predominating conformation of the nuclear DNA is the B-form. Evidence for this are the strong line at 1,094 cm^{-1}, due to the PO_2^- symmetric stretching vibration of the DNA backbone; the line at 833 cm^{-1}, belonging to a ribose-phosphate vibration of B-form DNA (but overlapping with the tyrosine doublet at ~830 and 853 cm^{-1}); and the positions of the ring-breathing vibrations of the DNA-bases (Table 1), which are consistent with a C'_2-endo-anti-sugar puckering.

No lines are found near ~807 and 870 cm^{-1}. This excludes the presence of large amounts of A-DNA or C-DNA. Small amounts of A-DNA have, however, been found in predominantly B-form DNAs (32). In spectra of nucleosomes (23) and reconstituted nucleosomes (34) indications were found that the complexed DNA possessed a slightly larger relative amount of A-DNA structure than free (B-form) DNA.

We have attempted to subject the spectral region around 810 cm^{-1} to a closer examination by means of a line fit procedure (42) to check for the presence of a hidden A-DNA line. However, the complexity of the spectrum is such that it prohibits a reasonable estimation of the background signal level. When the background parameters were included in the fit the resulting background signal level was strongly dependent on the number of lines used to fit the spectrum. Therefore no further information about the presence of A-DNA structure in the granulocyte nucleus could be obtained.

Z-DNA possesses a characteristic guanine vibration at ~625 cm^{-1} (43). The weak line at 623 cm^{-1} in the nucleus spectum is, however, most likely due to a phenylalanine vibration.

Our conclusion is therefore that from the spectrum of Fig. 1 no evidence can be obtained for the presence of non-B-form DNA structures in the nuclei of granulocytes.

Protein secondary structure

Information about protein secondary structure can be derived from the Amide I and Amide III spectral region (Table 1) (2, 44, 61). The maximum intensity of the Amide I band is found at 1,659 cm^{-1}. This is in between the positions where signal contributions originating from α-helix (~1,645–1,660 cm^{-1}) and random coil (~1,660–1,670 cm^{-1}) protein domains are expected. β-sheet signal contributions would have been expected at higher wavenumbers (~1,665–1,680 cm^{-1}). The only overlapping DNA signal in this region is due to carbonyl stretching vibrations of thymine, centered around 1,670 cm^{-1} (33) (see Fig. 2 *B*). The Amide III region is severely overlapping with DNA-base vibrations. Therefore not much information can be derived from this part of the spectrum. However, from the fact that a strong line below 1,240 cm^{-1} is absent it follows that only minor amounts of β-sheet structure are present. An extra

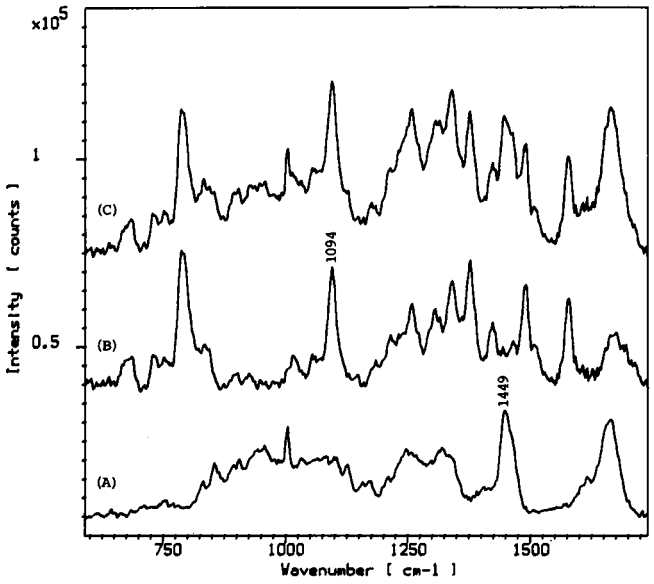

FIGURE 2 (*A*) Raman spectrum of a 47 mg/ml CT-histone II-AS solution in PBS. Laser power: 12 mW (660 nm), measuring time: 90 min (6 × 15 min). (*B*) Raman spectrum of an 18 mg/ml CT-DNA solution in PBS. Laser power 12 mW, measuring time: 60 min (4 × 15 min). (*C*) Sum spectrum *A* + *B*. The intensity scale is for the DNA spectrum. Spectrum *A* has been scaled in such a way that the product of sample concentration and measuring time is the same as for *B*. Spectrum *C* is therefore representative of a DNA-protein solution with equal amounts (weight) of DNA and protein.

indication for the presence of large amounts of α-helix structure comes from the high intensity of the C-C skeletal mode at 936 cm^{-1} (2). It is clear therefore that the proteins in the nucleus possess predominantly α-helix and random coil domains. These findings are in accordance with Raman spectroscopic data obtained from isolated nucleosomes, nucleosome cores, and from isolated Calf Thymus and chicken erythrocyte chromatin containing little or no nonhistone proteins (NHP) (26–28). As demonstrated below NHP is abundantly present in the nuclei of granulocytes. Therefore it can be concluded that like the histones these NHPs possess mainly α-helical and random coil domains.

DNA-protein ratio and NHP-histone protein ratio

The weight ratio DNA/histone protein in eukaryotic cell nuclei is ~1:1. The relative amount of nuclear NHP is strongly dependent on the type of cell. DNA/NHP weight ratios of the order of 0.05–1 have been found (45, 46).

In Fig. 2 spectra obtained from a CT-histone solution (*A*) and a CT-DNA solution (*B*) are shown, scaled in such a way that the product of measuring time and sample concentration is the same for both spectra. Their sum spectrum (Fig. 2 *C*) is therefore representative of a sample with a 1:1 DNA-protein ratio (as in nucleosomes).

Comparison of Fig. 2 *C* with the nucleus spectrum of Fig. 1 thus immediately shows that a large amount of NHP must be present in the granulocyte nuclei. We have made an estimation of the DNA-protein ratio in the granulocyte nucleus using the 1,094 cm^{-1} line in the nucleus spectrum as a marker for DNA concentration and the 1,449 cm^{-1} line as a marker for protein concentration (see Materials and Methods). The result is given in Table 2. The histone-NHP ratio follows directly from this result.

Cytoplasmic spectra. Spectra obtained from cytoplasmic regions of neutrophilic, eosinophilic, and basophilic granulocytes are shown in Figs. 3, 5, and 6. Contrary to the nuclear spectra, they differ dramatically.

Neutrophilic granulocytes

Fig. 3 *A* shows the Raman spectrum obtained of the cytoplasm of neutrophilic granulocytes. Strong signal contributions of MPO are present, as is clear from the spectrum of the purified enzyme shown in Fig. 3 *B*. MPO is a dimeric protein containing two covalently bound active site heme groups (47, 48). Its optical absorption spectrum is shown in Fig. 4. The MPO spectrum of Fig. 3 *B* strongly resembles, but is not identical to, resonance Raman (RR) spectra of the enzyme obtained with laser excitation in the absorption (Soret) band centered at 428 nm (47, 49). Strong lines present in the RR-spectra at 675 and 1,551 cm^{-1} are absent from the MPO and neutrophilic granulocyte spectra excited at 660 nm. On the other hand the strong lines at 982, 1,502, and 1,542 cm^{-1} in the spectra of Fig. 3 are absent or very weak (982 cm^{-1}) in the RR spectra.

Electron paramagnetic resonance studies showed MPO to possess high spin ferric heme groups (50). The RR studies confirmed this and moreover showed that the MPO heme groups are most likely chlorins (47, 49). Their low symmetry inhibits vibrational coupling. Resonance enhancement occurs therefore via direct electronic transition. The excitation profiles in the interval 300–600 nm for heme group vibrational modes shown in reference 47 all have a virtually identical wavelength dependence. There is a strong enhancement (up to 120 times) upon excitation in the Soret band and no or very

TABLE 2 DNA-Protein ratio and Histone-NHP ratio in the nucleus of a human granulocyte

DNA:Protein	1:2.3 (± 0.4)
Histone:NHP	1:1.3 (± 0.4)

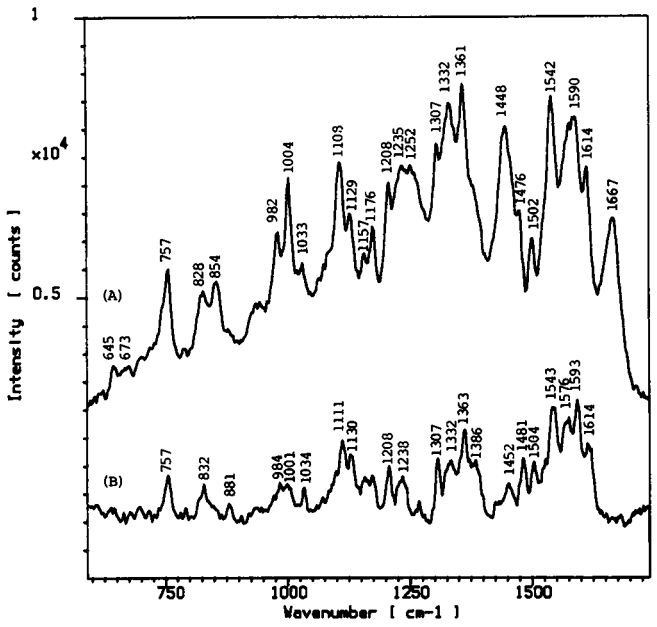

FIGURE 3 (*A*) Neutrophilic granulocyte cytoplasmic Raman spectrum averaged over five measurements of different cells. Laser power: 6 mW (660 nm), measuring time: 30 s per cell. (*B*) Raman spectrum of isolated native (oxidized) human MPO. Sample concentration: 230 $mM \cdot l^{-1}$ in a 200 mM phosphate buffer, Laserpower: 10 mW (660 nm), total measuring time 1,800 s (18 × 100 s). A high, fluorescent background due to sample impurities was removed by means of subtraction of an appropriate fifth-order polynome.

little enhancement upon excitation in the visible absorption band at 568 nm. Based on these data the occurrence of new lines in the spectra presented here can only be explained by the fact that they are not or only weakly

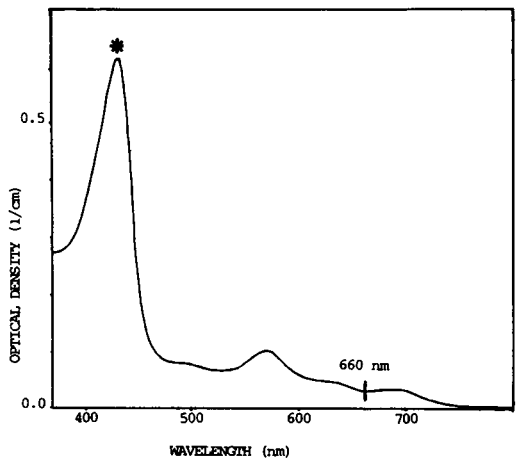

FIGURE 4 Absorption spectrum of native human MPO ($\sim 7\ mM \cdot l^{-1}$) in a 200 mM phosphate buffer. Asterisk denotes Soret-band.

enhanced upon excitation in the Soret band and become visible here because of the reduced enhancement of other modes upon 660 nm excitation. This explanation can be reversed to account for the disappearance of lines, i.e., modes which are very strongly enhanced upon excitation in the Soret band will show the largest relative decrease in intensity upon 660 nm excitation. However, this does not provide a completely satisfactory explanation because it cannot account for the fact that, e.g., the lines at 1,362 and 1,590 cm^{-1} are still present in the spectra of Fig. 3 while the 1,551 cm^{-1} line has disappeared. All three lines are of the same intensity in the RR spectra (47, 49) and have equal enhancement factors upon Soret band excitation (47). It would therefore be of interest to extend the excitation profiles given in reference 47 from 600 to 700 nm so that they include the weak absorption bands that are present at 626 and 684 nm (see Fig. 4).

The strong signal contributions of MPO prohibit identification of other compounds present in the cytoplasmic granules. Only some general information can be obtained from the amide I region. Its position suggests that the proteins that are present largely consist of random coil domains.

Eosinophilic granulocytes

The major constituents of eosinophil secondary granules are Major Basic Protein and EPO. On average an amount of 5 pg of Major Basic Protein and 15 pg of EPO per cell is found (16). This means that the concentrations of these compounds in granules are as high as 25 mg/ml for Major Basic Protein and 75 mg/ml for EPO. EPO possesses a ferric heme prosthetic group (51). The eosinophilic granulocyte cytoplasmic spectra are characterized by a very high signal intensity (e.g., >3 times higher than found for neutrophilic granulocytes, with the same incident laser power and measuring time). Nearly all of this signal comes from the secondary granules. This is evident from a comparison of spectra A and B in Fig. 5.

Spectrum 5*A*, averaged over 10 measurements on different cells, was obtained from cytoplasmic regions filled with granules. Comparing Fig. 5*A* with published RR spectra of EPO obtained under 406.7 and 514.5 nm excitation (52) makes clear that the intense lines from the granules are due to EPO. The laser excitation wavelength may play a larger role here in the selective enhancement of vibrational modes than in the case of MPO because the EPO prosthetic group is a protoheme of high symmetry, allowing resonance enhancement through vibronic coupling. The presence of anomalously polarized Raman lines in the RR spectrum of EPO, found upon excitation at 514.5 nm is evidence of this (52). It explains why, e.g., the strong line at 1,365 cm^{-1}

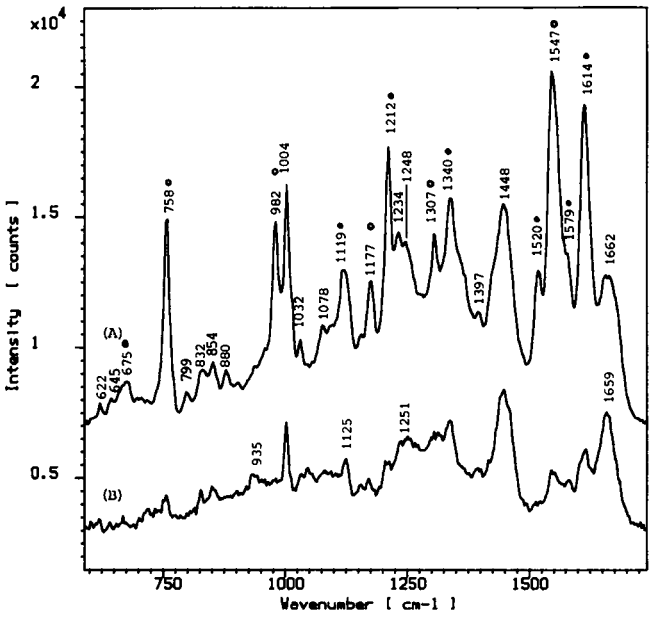

FIGURE 5 Eosinophilic granulocyte cytoplasmic Raman spectra. (*A*) Cytoplasmic regions with many granules. Spectrum averaged over 10 measurements of different cells. Laser power 6 mW (660 nm), measuring time: 30 s per cell. .: EPO line (52) o: line tentatively assigned to EPO. 758, 1,177, 1,307 cm^{-1}: shifted + 7 cm^{-1} relative to position in reference 52. 982, 1,547 cm^{-1}, see text. (*B*) Cytoplasmic region with few granules. Sum of two measurements. At the start of the measurements there were no granule(s) in the laser focus. Laser power: 6 mW (660 nm), measuring time: 30 s per measurement.

found in the spectra excited at 406.7 nm (in the Soret band) is already much reduced in intensity under 514.5 nm excitation (52) and only present as a shoulder in Fig. 5 *A*. It may also account for the fact that a line at 1,560 cm^{-1} in the spectra in reference 52 is not found in the present spectra and for the fact that a line at 1,548 cm^{-1} has appeared here which is absent from the spectra in reference 52. The appearance and disappearance of lines at 1,548 and 1,560 cm^{-1}, respectively, is an observation very similar to the one made for MPO. Another similarity with the results of MPO is the fact that in our spectra the 982 cm^{-1} line is strong, while it is very weak in the spectra in reference 52.

Even more so than in the case of MPO in neutrophilic granulocytes the signal contributions of EPO dominate the spectrum to an extent that it will be difficult to obtain any information about other cytoplasmic components.

Basophilic granulocytes

Spectra obtained from the cytoplasmic region of basophilic granulocytes showed large qualitative and quantitative variations. The spectra could roughly be divided into two groups, representatives of which are shown in Fig. 6 *A* and *B*. As described in Materials and Methods, enriched basophil fractions where obtained by fluorescence activated cell sorting. The fluorescent labeling of the basophilic granulocytes did not lead to a higher background signal level in comparison with Raman measurements of unlabeled cells. (For unlabeled cells the intensity ratio Raman signal/background signal [after subtraction of the water-Raman signal] for strong Raman lines is typically >2:1.) Fig. 6 *C* shows the spectrum obtained of the stock solution of the fluorescein conjugated human IgE antiserum, which was used to label the basophils. Comparison of Figs. 6 *A–C*, e.g., with respect to the line at 986 cm^{-1} in spectrum *C*, shows that no antiserum-fluorescein signal contributions are present in the basophil spectra. We have compared spectra 6*A* and 6*B* with published spectra of heparin (53) and histamine (54), two of the main constituents of the basophilic granulocyte cytoplasmic granules (18), but found little similarity. This may be due to the fact that these compounds are stored in the granules in a form different from the heparin samples used in reference 53 and the commercial histamine (Eastman Kodak) used in reference 54. Heparins are a family of compounds with considerable variation in physical and biological proper-

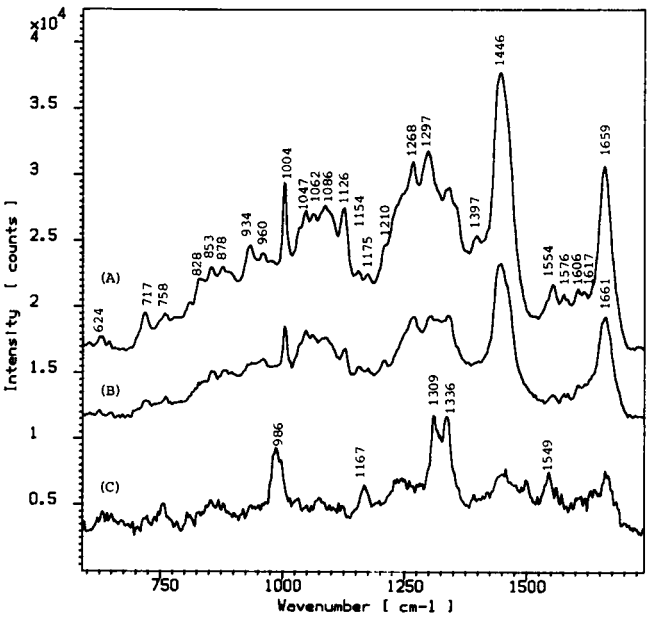

FIGURE 6 (*A, B*) Basophilic granulocyte cytoplasmic Raman spectra. Averages of (*A*) four and (*B*) five measurements of different cells. Laser power: 6 mW (660 nm), measuring time 150 s per measurement. (*C*) Raman spectrum of the stock solution of fluorescein conjugated human IgE antiserum. For labeling of basophils a 100 times diluted solution was used. Laser power: 12 mW measuring time 10 min. A background signal level of 20,000 counts was subtracted from the spectrum.

ties. A marked variability exists among heparins of different species (59). A common feature of the Raman spectra of glycosaminoglycans is a strong line at ~1,040–1,070 cm^{-1} due to a symmetric S-O stretching vibration (53, 55). No clearly distinguishable line is present in the basophilic granulocyte spectra. It may, however, be hidden in the broad band of overlapping Raman lines found in this spectral region.

The spectra, especially Fig. 6 *A* do bear some resemblance to spectra of human erythrocyte ghosts (32, 56, 57) suggesting the presence of phospholipid signal contributions at 1,297 and 1,268 cm^{-1}. These could also account for the position of the CH_2 bending vibration line at 1,446 cm^{-1} which is lower than usually found for proteins (~1,449–1,451 cm^{-1}), and for part of the signal found between 1,040 and 1,130 cm^{-1}. Phospholipid signal contributions could possibly originate from the dense multiple concentric membranous arrays found in the cytoplasmic granules (58). The fact that these granules are bound to the cell membrane (17) may (partly) explain the low reproducibility of basophilic granulocyte cytoplasmic spectra, because it implies that the distribution of granules in the basophilic granulocyte cytoplasm is very inhomogeneous.

CONCLUSIONS

High quality Raman spectra were obtained from nuclei and cytoplasmic regions of single living human granulocytes. It was found that the nuclear spectra of neutrophilic, eosinophilic, and basophilic granulocytes were indistinguishable, and contained only clear signal contributions of DNA and proteins. RNA or phospholipid contributions were not discernable.

The B-form was found to be the predominant DNA-conformation. This does not imply that other DNA forms are absent. The complexity of the spectra is such, however, that alternative DNA conformations, involving < ~5–10% of the total DNA, will be hard to detect. The most fortunate situation would be when differences in DNA secondary structure would exist between different nuclear domains. Difference Raman spectroscopy could then be applied which could lower the level of detectability of non-B-form DNA. The nuclear proteins possess predominantly α-helical and random coil domains. The DNA-protein ratio (w/w) was determined to be 1:2.3 (±0.4) and from this followed that the histone-NHP ratio is 1:1.3 (±0.4). A (thus far unassigned) line was found at 1,048 cm^{-1} in the nuclear spectra that has not been observed before in spectra of DNA, chromatin, or chromosomes. It was the only line which showed large variations in intensity.

The neutrophilic and eosinophilic granulocyte cytoplasmic spectra contained large signal contributions of MPO and EPO, respectively. They showed that these enzymes can be studied in situ by means of Raman spectroscopy. An exciting prospect is the possibility to monitor the processes of phagocytosis and digestion of foreign objects. The peroxidases can then be studied in their active state in the cell. It will probably be advantageous then to shift the laser excitation wavelength to ~750 nm. In that way absorption of laser light by the enzymes, which in the present work limited the measuring time to 30 s, is avoided.

The basophilic granulocyte cytoplasmic spectra appear to contain large phospholipid signal contributions, but the spectra and their large cell-to-cell variation remain puzzling.

The fact that Raman spectra could be obtained from basophilic granulocytes after immuno labeling with fluorescein conjugated antiserum is very valuable. It offers a method to select specific cell populations for Raman spectroscopic analysis. The combination of fluorescence activated cell sorting and Raman microspectroscopy is presently used to study different lymphocyte subclasses.

The authors wish to thank Dr. R. Wever of the University of Amsterdam for helpful suggestions and a sample of MPO, W. Reichart for courier services, Y. M. Kraan and K. Radošević for analytical assistance, and Dr. E. F. Knol of the Central Laboratory of the Netherlands Red Cross Blood Transfusion Service for helpful advice.

Received for publication 25 February 1991 and in final form 30 May 1991.

REFERENCES

1. Spiro, T. G. (ed.). 1987–1988. *Biological Applications of Raman Spectroscopy.* John Wiley & Sons, New York. Vols. 1–3.
2. Tu, A. T. 1987. *Raman Spectroscopy in Biology: Principles and Applications.* John Wiley & Sons, New York. 448 pp.
3. Clark, R. J. H. and R. E. Hester. (eds.) 1986. *Advances in Spectroscopy.* Spectroscopy of Biological Systems, Heyden, London. 13. 547 pp.
4. Kubasek, W. L., Y. Wang, G. A. Thomas, T. W. Patapoff, K.-H. Schoenwaelder, J. H. Van der Sande, and W. L. Peticolas. 1986. Raman spectra of the model B-DNA oligomer d(CGCCAATTCGCG)$_2$, and of the DNA in living salmon sperm show that both have very similar B-type conformations. *Biochemistry.* 25:7440–7445.
5. Barry, B., and R. Mathies. 1982. Resonance Raman microscopy of rod and cone receptors. *J. Cell Biol.* 94:479–482.
6. Jeannesson, P., J. F. Angiboust, J. C. Jardillier, and M. Manfait. 1986. Biomedical applications of Raman spectroscopy: investigations of molecular and cellular systems. *In Proceedings IEEE/8th Annual Conference of the Engineering in Medicine and Biology Society.* 1404–1406.
7. Dalterio, R. A., W. H. Nelson, D. Britt, J. F. Sperry, and F. J.

Purcell. 1986. A resonance Raman microprobe study of chromobacteria in water. *Appl. Spectrosc.* 40:271–272.

8. Puppels, G. J., F. F. M. De Mul, C. Otto, J. Greve, M. Robert-Nicoud, D. J Arndt-Jovin, and T. M. Jovin. 1990. Studying single living cells and chromosomes by confocal Raman microspectroscopy. *Nature (Lond.).* 347:301–303.
9. Puppels, G. J., W. Colier, J. H. F. Olminkhof, C. Otto, F. F. M. De Mul, and J. Greve. 1991. Description and performance of a highly sensitive confocal Raman microspectrometer. *J. Raman Spectrosc.* 22:217–225.
10. Bessis, M. 1973. Living Blood Cells and their Ultrastructure. Springer, Berlin.
11. Keele, C. A., and E. Neil. (eds.) 1971. Samson Wright's Applied Physiology. 12th ed. Oxord Medical Publications, Oxford.
12. Schultz, J. and K. Kaminker. 1962. Myeloperoxidase of the leucocyte of normal human blood. 1: Content and localization. *Arch. Biochem. Biophys.* 96:465–467.
13. Parker, C. W. 1984. Effector mechanisms of immunity. Mediators: release and function. *In Fundamental Immunology.* Paul, W. E., editor. Raven Press, New York. 697–747.
14. Klebanoff, S. J., and R. A. Clark. 1978. *The Neutrophil: Function and Disorders.* North-Holland, Amsterdam.
15. Butterfield, J. H., D. E. Maddox, and G. J. Gleich. 1984. The eosinophil leukocyte: maturation and function. *Clin. Immunol. Rev.* 2(2):187–306.
16. Gleich, G. J., and C. R. Adophson. 1986. The eosinophil leukocyte: structure and function. *In Advances in Immunology* 39. Dixon, F. J., editor. Academic Press, Orlando. 177–253.
17. Galli, S. J., and H. F. Dvorak. 1978. Basophils and mast cells: structure, function, and role in hypersensitivity. *In Cellular, Molecular and Clinical Aspects of Allergic Disorders.* Gupta, S., Good, R. A. editors. Plenum Medical Book Company, New York.
18. Ho, P. C., R. A. Lewis, F. Austen, and R. P. Orange. 1978. Mediators of immediate hypersensitivity. *In Cellular, Molecular and Clinical Aspects of Allergical Disorders.* Grupta, S., Good, R. A., editors. Plenum Medical Book Company, New York. 179–228.
19. Terstappen, L. W. M. M., B. G. De Grooth, G. M. J. Nolten, C. H. H. Ten Napel, W. Van Berkel, and J. Greve. 1986. Physical discrimination between human T lymphocyte subpopulations by means of light scattering, revealing two populations of T8 positive cells. *Cytometry.* 7:178–183.
20. Ackermann, S. J., G. M. Kephart, T. M. Habermann, P. R. Greipp, and G. J. Gleich. 1983. Localization of eosinophil major basic protein in human basophils. *J. Exp. Med.* 158:946–961.
21. Terstappen, L. W. M. M., R. A. Mickaels, R. Dost, and M. R. Loken. 1990. Increased light scattering resolution facilitates multidimensional flow cytometric analysis. *Cytometry.* 11:506–512.
22. Begemann, H., and J. Rastetter. 1979. *Atlas of Clinical Hematology.* 3rd. ed. Springer, Berlin.
23. Bakkenist, A. R. J., R. Wever, R. Vulsma, H. Plat, and B. F. Van Gelder. 1978. Isolation procedure and some properties of myeloperoxidase from human leucocytes. *Biochim. Biophys. Acta.* 524:45–54.
24. Parks, D. R., V. M. Bryan, V. M. Oi, V. T. Oi, and L. A. Herzenberg. 1979. Antigen specific identification and cloning of hybridomas with a fluorescence activated cell sorter (FACS). *Proc. Natl. Acad. Sci. USA.* 76:1962–1966.
25. Peterson, G. L. 1979. Review of the Folin phenol protein quantitation method of Lowry, Rosebourgh, Farr and Randall. *Anal. Biochem.* 100:201–220.
26. Thomas, Jr., G. J., B. Prescott, and D. E. Olins. 1977. Secondary structure of histones and DNA in chromatin. *Science (Wash. DC).* 197:385–388.
27. Hayashi, H., Y. Nishimura, M. Katahira, and M. Tsuboi. 1986. The structure of nucleosome core particles as revealed by difference Raman spectroscopy. *Nucl. Acids Res.* 14(6):2583–2596.
28. Savoie, R., J.-J. Jutier, S. Alex, P. Nadeau, and P. N. Lewis. 1985. Laser Raman spectra of calf thymus chromatin and its constituents. *Biophys. J.* 47:451–459.
29. Prescott, B., C. H. Chou, and G. J. Thomas. Jr. 1976. A Raman spectroscopic study of complexes of polylysine with deoxyribonucleic acid and polyriboadenylic acid. *J. Phys. Chem.* 80:1164–1171.
30. Mansy, S., S. K. Engstrom, and W. L. Peticolas. 1976. Laser Raman identification of an interaction site on DNA for arginine containing histones in chromatin. *Biochem. Biophys. Res. Commun.* 68(4):1242–1247.
31. Thomas. Jr., G. J. and K. A. Hartman. 1973. Raman studies of nucleic acids VIII: estimation of RNA secondary structure from Raman scattering by phosphate-group vibrations. *Biochim. Biophys. Acta.* 311–322.
32. Wallach, D. F. H., and S. P. Verma. 1975. Raman and resonance-Raman scattering by erythrocyte ghosts. *Biochim. Biophys. Acta.* 382:542–551.
33. Erfurth, S., and W. L. Peticolas. 1975. Melting and premelting phenomenon in DNA by laser Raman scattering. *Biopolymers.* 14:247–264.
34. Tsuboi, M., S. Takahashi, and I. Harada. 1973. Infrared and Raman spectra of nucleic acids-vibrations in the base residues. *In Physico-chemical Properties of Nucleic Acids.* Duchesne, J., editor. Academic Press, New York. 2:91–145.
35. Goodwin, D. C., and J. Brahms. 1978. Form of DNA and the nature of interactions with proteins in chromatin. *Nucl. Acids Res.* 5(3):835–850.
36. Thomas, Jr., G. J., B. Prescott, and M. G. Hamilton. 1980. Raman spectra and conformational properties of ribosomes during various stages of disassembly. *Biochemistry.* 19:3604–3613.
37. Thomas, Jr., G. J., J. M. Benevides, and B. Prescott. 1986. DNA and RNA structures in crystals, fibers, and solutions by Raman spectroscopy with applications to nucleoproteins. *In Biomolecular Stereodynamics IV.* Sarma, R. H., and M. H. Sarma, editors. Adenine Press, Guilderland, NY. 227–253.
38. Prescott, B., W. Steinmetz, and G. J. Thomas Jr. 1984. Characterization of DNA structures by laser Raman spectroscopy. *Biopolymers.* 23:235–256.
39. Wartell, R. M., and J. T. Harrell. 1986. Characteristics and variations of B-type DNA conformations in solution: a quantitative analysis of Raman band intensities of eight DNAs. *Biochemistry.* 25:2664–2671.
40. Thomas, Jr., G. J., B. Prescott, and L. A. Day. 1983. Structure similarity, difference and variability in the filamentous virusses fd, If1, IKe, Pf1 and Xf. *J. Mol. Biol.* 165:321–356.
41. Brahms, S., S. K. Brahmachari, N. Angelier, and J. G. Brahms. 1981. Conformation of DNA in chromatin reconstituted from poly [d(A-T)] and the core histones. *Nucl. Acids Res.* 9(19):4879–4893.
42. De Mul, F. F. M., H. B. G. Ten Have, C. Otto, and J. Greve. 1990. The MCGA (multiple cubic gradient approximation) method

for the analysis of Raman spectra. *J. Raman Spectrosc.* 21:725–736.

43. Peticolas, W. L., W. L. Kubasek, G. A. Thomas, and M. Tsuboi. 1987. Nucleic Acids. *In Biological Applications of Raman Spectroscopy.* Spiro, T. G., editor. 1:81–134.
44. Lippert, J. L., D. Tyminski, and P. J. Desmeules. 1976. Determination of the secondary structure of proteins by laser Raman spectroscopy. *J. Am. Chem. Soc.* 98:7075–7080.
45. Mathews, C. K., and K. E. Van Holde. 1990. *Biochemistry.* Benjamin/Cummings, Redwood, CA. 1003–1004.
46. Bradbury, E. M., N. Maclean, and H. R. Matthews. 1981. *DNA, Chromatin and Chromosomes.* Blackwell, Oxford.
47. Sibbett, S. S., and J. K. Hurst. 1985. Structural analysis of myeloperoxidase by resonance Raman spectroscopy. *Biochemistry.* 23:3007–3013.
48. Bolscher, B. G. J. M. 1986. Spectroscopic and structural properties of mammalian haloperoxidases. PhD. thesis, University of Amsterdam, the Netherlands. 117 pp.
49. Babcock, G. T., R. T. Ingle, W. A. Oertling, J. C. Davis, B. A. Averill, C. L. Hulse, D. J. Stufkens, B. G. J. M. Bolscher, and R. Wever. 1985. Raman characterization of human leukocyte myeloperoxidase and bovine spleen green haemoprotein. Insight into chromophore structure and evidence that the chromophores of myeloperoxidase are equivalent. *Biochim. Biophys. Acta.* 828:58–66.
50. Wever, R., D. Roos, R. S. Weening, T. Vulsma, and B. F. Van Gelder. 1976. An EPR study of myeloperoxidase in human granulocytes. *Biochim. Biophys. Acta.* 421:328–333.

50*a*. Ehrenberg, A. 1962. Electron spin resonance absorption by some hemoproteins. *Ark. Kemi.* 19:119–128.

50*b*. Schultz, J., H. Snyder, N.-C. Wu, N. Berger, and M. J. Bonner. 1972. Chemical nature and biological activity of myeloperoxidase. *In The Molecular Basis of Electron Transport.* Schultz, J., B. F. Cameron, editors. Academic Press, New York. 301–325.

51. Wever, R., M. N. Hamers, R. S. Weening, and D. Roos. 1980. Characterization of the peroxidase in human eosinophils. *Eur. J. Biochem.* 108:491–495.
52. Sibbett, S. S., S. J. Klebanoff, and J. K. Hurst. 1985. Resonance Raman characterization of the heme prosthetic group in eosinophil peroxidase. *FEBS (Fed. Eur. Biochem. Soc.) Lett.* 2911:271–275.
53. Cabassi, F., B. Casu, and A. S. Perlin. 1978. Infrared absorption and Raman scattering of sulfate groups of heparin and related glucosaminoglycans in aqueous solution. *Carbohydr. Res.* 63:1–11.
54. Itabashi, M., K. Shoji, and K. Itoh. 1982. Raman spectra of copper (II)-histamine. (1:2) and nickel (II)-histamine (1:2) aqueous solutions. *Inorg. Chem.* 21(9):3485–3489.
55. Bansil, R., I. V. Yannis, and H. E. Stanley. 1978. Raman spectroscopy: a structural probe of glycosaminoglycans. *Biochim. Biophys. Acta.* 541: 535–542.
56. Goheen, S. C., T. H. Gilman, J. W. Kaufmann, and J. E. Garvin. 1977. The effect on Raman spectra of extraction of peripheral proteins from human erythrocyte membranes. *Biochem. Biophys. Res. Commun.* 79(3):805–814.
57. Lippert, J. L., L. E. Gorczyca, and G. Meiklejohn. 1975. A laser-Raman investigation of phospholipid and protein configurations in hemoglobin free erythrocyte ghosts. *Biochim. Biophys. Acta.* 382:51–57.
58. Dvorak, A. M., and S. J. Ackerman. 1989. Ultrastructural localization of the Charcot-Leyden crystal protein (lysophospholipase) to granules and intragranular crystals in mature human basophils. *Lab. Invest.* 60(4):557–567.
59. Sigma Chemical Company, product catalogue. 1991. St. Louis, MO.
60. Yu, N.-T., D. C. Denagel, D. J.-Y. Ho, and J. F. R. Kuck. 1987. Ocular Lenses. *In Biological Applications of Raman Spectroscopy.* (Spiro; T. G., editor. John Wiley & Sons, New York. 1:47–80.
61. Carey, P. R. 1982. *Biochemical Applications of Raman and Resonance Raman Spectroscopies.* Academic Press, New York. 71–98.
62. Puppels, G. J., J. H. F. Olminkhof, G. M. J. Segers-Nolten, C. Otto, F. F. M. De Mul, and J. Greve. 1991. Laser irradiation and Raman spectroscopy of single living cells and chromosomes: Sample degradation occurs with 514.5 nm but not with 660 nm laser light. *Exp. Cell. Res.* In press.
63. Stump, R. F., G. G. Deanin, J. M. Oliver, and J. A. Sheluutt. 1987. Heme-linked ionizations of myeloperoxidase detected by Raman difference. *Biophys. J.* 51:605–610.
64. Ikeda-Saito, M., P. V. Argade, and D. L. Rousseau. 1985. Resonance Raman evidence of chloride binding to the heme iron in myeloperoxidase. *FEBS (Fed. Eur. Biochem. Soc.) Lett.* 184:52–55.